

THE TRANSITION TO TURBULENCE OF THE TORSIONAL COUETTE FLOW

Anne Cros and Patrice Le Gal

*Institut de Recherche sur les Phénomènes Hors Equilibre,
49, rue F. Joliot-Curie, 13384, Marseille, cédex 13, France*
legal@irphe.univ-mrs.fr

Abstract This work is devoted to the experimental study of the transition to turbulence of a flow confined in a narrow gap between a rotating and a stationary disk. When the fluid layer thickness is of the same order of magnitude as the boundary layer depth, the azimuthal velocity axial gradient is nearly constant and this rotating disk flow is a torsional Couette flow. As in the plane Couette flow or the cylindrical Couette flow, transition to turbulence occurs via the appearance of turbulent domains inside a laminar background. Nevertheless, we show that in the rotating disk case, the nucleation of turbulent spirals is connected to the birth of structural defects in a periodic underlying spiral roll pattern.

Keywords: Couette flow, rotating disk flow, defect turbulence, by-pass transition

Introduction

Transition to turbulence in extended systems can be induced by the erratic nucleation of defects in periodical patterns. This is the case in Rayleigh-Bénard convection [1] or in Taylor-Dean system [2] for instance. Topological defects in wave patterns have also been identified in numerical solutions of coupled Landau-Newell type equations [3] or of the complex Ginzburg-Landau equation (CGLE) [4, 5] and the mechanism for transition from phase to defect chaos has been identified by Couillet et al. [6]. In our work, a primary instability creates a periodic laminar spiral wave pattern in the torsional Couette flow confined between a rotating and a stationary disk [7, 8]. As the rotation rate of the disk is increased, some defects appear through the local disappearance of a spiral (a dislocation), or through the connection of two systems of spirals with different orientations (a grain boundary). Then as the control parameter is further increased, the number of these defects increases, and spatially localized chaotic regions develop under the form of turbulent spirals (TS). In this paper, we first describe the appearance of the disorder (Defect Turbulence) in the periodic pattern until the first TS waves appear. Then, the lifetime of these

turbulent structures grows and they form permanent turbulent spirals arranged nearly periodically all around the disks. We will thus describe in the second part of this article this transitional process in the framework of spatiotemporal intermittency (STI). This mechanism involves a mixed state of turbulent patches and laminar domains, which coexist for the same values of the control parameter. This kind of scenario has been observed in different systems [9–11]. Several experiments have also described this mechanism of transition to turbulence. In particular, it was studied in Rayleigh-Bénard convection in annular and rectangular geometries [12, 13] and in the Taylor-Dean [14] or the Taylor-Couette systems [15]. In all these experiments, the transition to turbulence via STI was described within the framework of critical phenomena. Pomeau [16] proposed in 1986 that the spatiotemporal intermittency scenario could be similar to a percolation process, where the disordered state would propagate into the laminar one via a contamination mechanism. In this case, the turbulent state would be the "active", or "contaminant" phase, while the laminar state would be the "absorbing", or the "passive" state. Although the critical exponents found in experiments take various values and do not correspond to those of percolation, we will keep this terminology to describe the first steps of the invasion process of the turbulence in our own system. In particular we will define a "percolation threshold" as the limit value of the control parameter for which the turbulent structures possess an infinite lifetime.

1. The rotating disk device

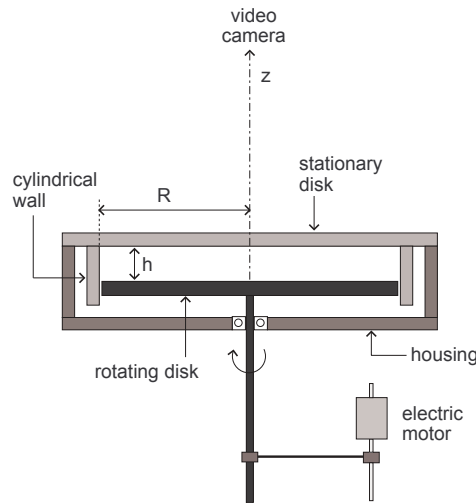


Figure 1. Rotating disk device.

The experimental device, presented in Figure 1, consists of a water-filled cylindrical casing in which the rotating disk is immersed. The top lid of the container plays the role of the stationary disk. The radius of the stainless steel disk is 140 mm and its thickness is 13 mm. It is painted in black to enhance visualizations which are realized with kalliroscope flakes. The drive shaft goes through the bottom of the tank and is connected to a d.c. electric motor whose rotating velocity can be varied from $\Omega = 0$ to 200 rpm with an accuracy better than 0.2%. The stationary disk is a 20 mm thick plexiglass plate, so that the flow can be observed through it. The distance between the rotating disk and the fixed one is set to 2 mm. A CCD video camera is placed on the rotation axis and can rotate if necessary with a velocity which can be adjusted in order to observe the waves in their rotating frame. This video camera is finally connected to a computer, and images can be captured in real time.

2. Transition to Defect Turbulence

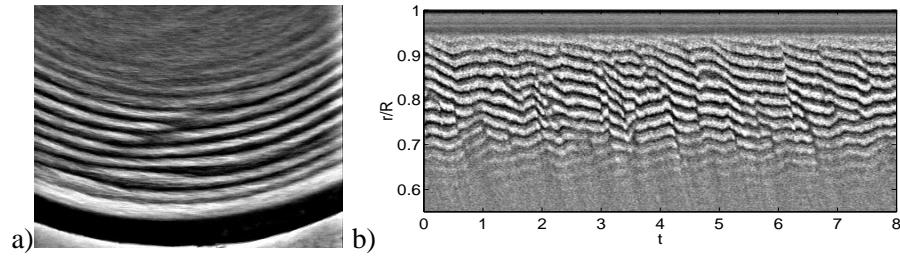


Figure 2. a) Defect in the spiral roll pattern. b) Space-time diagram along a radius

Figure 2-a) shows a typical defect of the laminar spiral pattern. We will describe the flow by the use of spatio-temporal diagrams which are realized

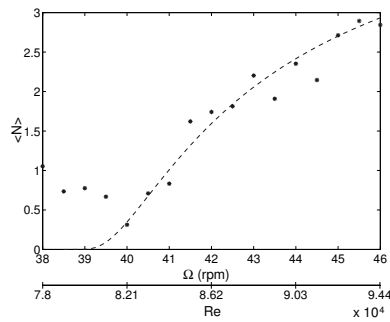


Figure 3. Total number of defects versus Reynolds number with a fit as proposed in [17]

along the radial direction. Figure 2-b) presents such a diagram where Defect Turbulence [6] can be observed. A statistical study of these defects shows that their occurrence obeys a Poisson law near their threshold. We observe also in Figure 3 that their number increases similarly to what is proposed by theoretical studies [17]. Our results are also in agreement with the interpretation that these defects are homoclinic orbits of a dynamical system nearby a saddle-node critical point [18]. As the rotation rate is further increased, the time duration separating two consecutive defects decreases dramatically and the defects are associated to strong amplitude modulations. A similarity with the “MAWs” of Brusch et al. [4] is striking. In fact, these modulations act as seeds for the turbulent spirals visualized in Figure 4-a).

3. Spatio-temporal Intermittency

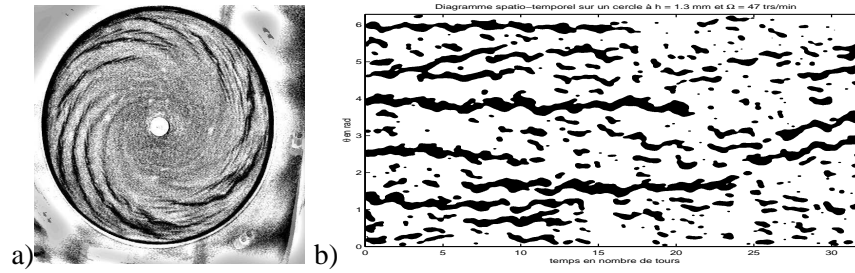


Figure 4. a) Visualization of the turbulent spirals. b) Space-time diagram (along a circle) showing the turbulent spirals (in black) inside the laminar flow (in white)

Very near their observation threshold, these turbulent structures that are the equivalents of the turbulent spirals of the cylindrical Couette flow (note that in spite of their traditional appellation, they are not spirals in this case but rather helices!) have a very short life time. As the rotation rate is further increased, this lifetime increases until a threshold is reached (the percolation threshold) where they finally form permanent turbulent spirals arranged nearly periodically all around a circumference. However, since the number of these turbulent spirals decreases with the rotational frequency, the transition to a fully turbulent regime is never achieved. Thus the turbulent fraction of the pattern saturates to a value close to 0.5. Figure 5 presents the evolution of this turbulent fraction with the Reynolds number. However, as it can be seen, this turbulent fraction presents a power law critical behavior with an exponent $\beta = 0.3$ near its threshold.

Another exponent of the transition can also be measured. As presented in Figure 6-a), the statistics of the length of the laminar domain follows an exponential law with a well defined characteristic length. The evolution of these

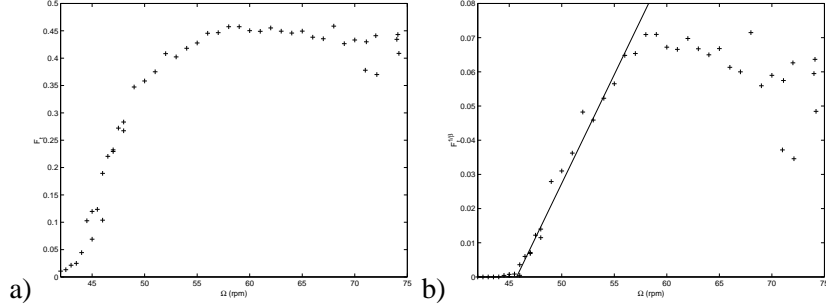


Figure 5. a) Evolution of the turbulent fraction versus Reynolds number. b) At threshold, an exponent $\beta = 0.3 \pm 0.01$ can be determined.

laminar domains lengths versus the Reynolds number presents a divergence with a power law with an exponent $\alpha = -\frac{1}{2}$ (see Figure 6-b). Thus, although the transition to turbulence is not completed, it appears that it really shares some features with Space-Time Intermittency [19]. Therefore, although a universal scenario is still lacking for this type of transition to turbulence, we note that values of both α and β agree with the measures of Daviaud et al. [12] in their convection experiments. Note also that the saturation of the turbulent fraction near 0.5 is reminiscent of the amazing periodization of turbulence in bands as discovered by Prigent et al. [20] in the plane and in the cylindrical Couette flow and reproduced numerically by Barkley and Tuckerman [21].

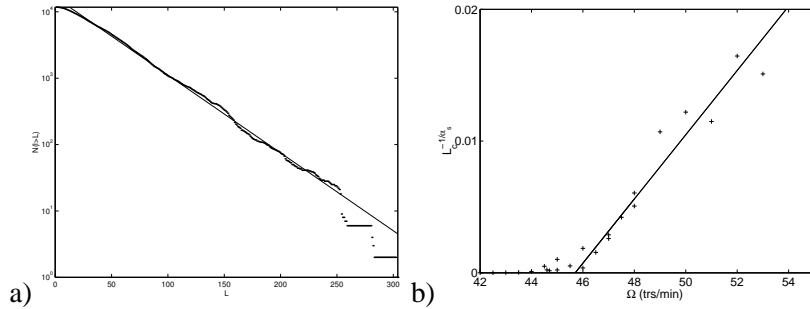


Figure 6. a) Exponential behavior of the histogram of the laminar lengths. b) Measure of the exponent $\alpha = -\frac{1}{2}$ of the critical behavior of the laminar length.

References

- [1] A. Pocheau, V. Croquette and P. Le Gal. (1985). "Turbulence in a Cylindrical Container of Argon near Threshold of Convection," Phys. Rev. Lett. 55, 1094 .

- [2] P. Bot and I. Mutabazi. (2000). "Dynamics of spatio-temporal defects in the Taylor-Dean system," *Eur. Phys. J. B* 13, 141 .
- [3] P. Coullet, C. Elphick, L. Gil and J. Lega. (1987). "Topological defects of wave patterns," *Phys. Rev. Lett.* 59, 884 .
- [4] L. Brusch , M.G. Zimmerman, M. van Hecke, M. Bar and A. Torcini. (2000). " Modulated amplitude waves and the transition from phase to defect chaos," *Phys. Rev. Lett.* 85, 86.
- [5] M. van Hecke. (1998). " Building Blocks of Spatiotemporal Intermittency," *Phys. Rev. Lett.* 80, 1896 .
- [6] P. Coullet, L. Gil and J. Lega. (1989). " Defect-mediated turbulence," *Phys. Rev. Lett.* 62(14), 1619.
- [7] A. Cros and P. Le Gal. (2002). "Spatio-temporal intermittency in the torsional Couette flow between a rotating and a stationary disk," *Phys. Fluids*, 14(11),3755.
- [8] A. Cros and P. Le Gal. (2004). "Defect turbulence in a spiral wave pattern in the torsional Couette flow," *Phys. Rev. E* 70, 016309.
- [9] H. Chaté, P. Manneville. (1987). "Intermittence spatio-temporelle et automates cellulaires probabilistes," *C.R. Acad. Sc. (Paris)* 304 II, 609.
- [10] H. Chaté, and P. Manneville (1988). "Spatiotemporal intermittency in coupled map lattices," *Physica D* 32, 409.
- [11] H. Chaté. (1994). "Spatiotemporal intermittency regimes of the one-dimensional complex Ginzburg-Landau equation," *Nonlinearity* 7, 185.
- [12] F. Daviaud, M. Bonetti and M. Dubois. (1990). " Transition to turbulence via spatio-temporal intermittency in one-dimensional Rayleigh-Bénard convection," *Phys. Rev. A*, 42, 3388.
- [13] S. Ciliberto, and P. Bigazzi. (1988). "Spatiotemporal intermittency in Rayleigh-Bénard convection," *Phys. Rev. Lett.* 60, 286.
- [14] M. M. Degen, I. Mutabazi, and C. D. Andereck. (1996). "Transition to weak turbulence via spatiotemporal intermittency in the Taylor-Dean system," *Phys. Rev. E*, 53, 3505.
- [15] P. W. Colovas and C. D. Andereck. (1997). "Turbulent bursting and spatiotemporal intermittency in the counterrotating Taylor-Couette system," *Phys. Rev. E*, 55, 2736.
- [16] Y. Pomeau. (1986). "Front motion, metastability and subcritical bifurcations in hydrodynamics," *Physica D* 23, 3.
- [17] B.I. Shraiman, A. Pumir A., W. Van Saarloos, P.C. Hohenberg, H. Chaté and M. Holen. (1992). "Spatio-temporal chaos in the one-dimensional complex Ginzburg-Landau equation," *Physica D*, 57, 241.
- [18] V.S. Afraimoich; and L.A. Bunimovich. (1995). " Density of defects and spatial entropy in extended systems," *Physica D* 80, 277.
- [19] H. Chaté and P. Manneville. (1987). "Transition to turbulence via spatio-temporal intermittency," *Phys. Rev. E*, 58, 112.
- [20] A. Prigent, G; Gregoire, H. Chaté, O. Dauchot and W. Van Saarloos. (2002). "Large-scale finite wavelength modulation within turbulent shear flows," *Phys. Rev. Lett* 89, 014501.
- [21] D. Barkley and L.S. Tuckerman.(2004). "Computational study of turbulent-laminar patterns in Couette flow," *Phys. Rev. Lett.* 94, 014502.